# Enzyme-activatable imaging probe reveals enhanced neutrophil elastase activity in tumors following photodynamic therapy

Soumya Mitra
Kshitij D. Modi
Thomas H. Foster

# Enzyme-activatable imaging probe reveals enhanced neutrophil elastase activity in tumors following photodynamic therapy

**Soumya Mitra,**[a] **Kshitij D. Modi,**[b] **and Thomas H. Foster**[a]
[a]University of Rochester Medical Center, Department of Imaging Sciences, Rochester, New York 14642
[b]PerkinElmer Inc., 850 Marina Village Parkway, Alameda, California 94501

**Abstract.** We demonstrate the use of an enzyme-activatable fluorogenic probe, Neutrophil Elastase 680 FAST (NE680), for *in vivo* imaging of neutrophil elastase (NE) activity in tumors subjected to photodynamic therapy (PDT). NE protease activity was assayed in SCC VII and EMT6 tumors established in C3H and BALB/c mice, respectively. Four nanomoles of NE680 was injected intravenously immediately following PDT irradiation. 5 h following administration of NE680, whole-mouse fluorescence imaging was performed. At this time point, levels of NE680 fluorescence were at least threefold greater in irradiated versus unirradiated SCC VII and EMT6 tumors sensitized with Photofrin. To compare possible photosensitizer-specific differences in therapy-induced elastase activity, EMT6 tumors were also subjected to 2-(1-hexyloxyethyl)-2-devinyl pyropheophorbide-a (HPPH)-PDT. NE levels measured in HPPH-PDT-treated tumors were twofold higher than in unirradiated controls. *Ex vivo* labeling of host cells using fluorophore-conjugated antibodies and confocal imaging were used to visualize $Gr1^+$ cells in Photofrin-PDT-treated EMT6 tumors. These data were compared with recently reported analysis of $Gr1^+$ cell accumulation in EMT6 tumors subjected to HPPH-PDT. The population density of infiltrating $Gr1^+$ cells in treated versus unirradiated drug-only control tumors suggests that the differential in NE680 fold enhancement observed in Photofrin versus HPPH treatment may be attributed to the significantly increased inflammatory response induced by Photofrin-PDT. The *in vivo* imaging of NE680, which is a fluorescent reporter of NE extracellular release caused by neutrophil activation, demonstrates that PDT results in increased NE levels in treated tumors, and the accumulation of the cleaved probe tracks qualitatively with the intratumor $Gr1^+$ cell population. © The Authors. Published by SPIE under a Creative Commons Attribution 3.0 Unported License. Distribution or reproduction of this work in whole or in part requires full attribution of the original publication, including its DOI. [DOI: 10.1117/1.JBO.18.10.101314]

## 1 Introduction

The inflammatory response elicited by photodynamic therapy (PDT) represents a complex and dynamic process characterized by elements of the innate immune system.[1,2] A hallmark of this host response is the massive recruitment of leukocytes, a significant fraction of which are neutrophils, to the treated tumor site.[3,4] This phenomenon has been observed with several different photosensitizers, including the US FDA approved Photofrin.[5] In our own work using *in vivo* imaging, we have recently demonstrated that PDT with the phthalocyanine photosensitizer, Pc4, or with 2-(1-hexyloxyethyl)-2-devinyl pyropheophorbide-a (HPPH), induces a significant increase in $Gr1^+$ cells in irradiated versus control EMT6 mouse mammary carcinoma tumors.[6,7] Several animal studies have also investigated the importance of intratumor neutrophil accumulation to the long-term curative outcome of PDT using selective depletion or inactivation of neutrophils and have demonstrated that the depletion of these effector cells results in a decrease of the PDT-mediated tumor cure rate.[3,8,9]

Neutrophil elastase (NE), proteinase 3 (PR3), and cathepsin G are three serine proteases stored in large quantities in neutrophil cytoplasmic azurophilic granules. These proteases are externalized in an active form during neutrophil activation at inflammatory sites, and recent studies have started to elucidate their contribution to the immune response. In this context, NE has received particular attention.[10,11] Although NE has been implicated in a variety of diseases due to its capacity to degrade the extracellular matrix, new findings provide compelling evidence that NE contributes considerably to the regulation of host functions.[12] A recent study reported that NE is involved in polymorphonuclear leukocyte-mediated host protection in a mouse model of *Pseudomonas aeruginosa*-induced pneumonia.[13] The study also demonstrated that extracellularly active NE has the capacity to induce mRNA expression of the proinflammatory cytokines tumor necrosis factor $\alpha$ (TNF-$\alpha$), macrophage inflammatory protein-2, and interleukin-6 (IL-6).

The growing recognition of the role of proteinases and proteolytic cascades in both the growth and metastasis of tumors has led to the development not only of therapeutic strategies using proteinase inhibitors but also of methods to detect and image tumors *in vivo* via tumor-associated proteolytic activities.[14–16] These selective protease probes belong to a family of imaging agents that are optically invisible or at least display reduced fluorescence when administered intravenously until

Address all correspondence to: Soumya Mitra, University of Rochester, Department of Imaging Sciences, 601 Elmwood Avenue, Box 648, Rochester, New York 14642. Tel: 585-275-3645; Fax: (585) 273-1033; E-mail: soumya .mitra@rochester.edu

activated by enzymatic cleavage at the disease site. This allows localization of fluorescence signal in areas of enzyme activity with low background in tissue regions that do not activate the probes. Thus, increased signal levels report enhanced proteolytic activity. Recently, several of these activatable imaging probes have been developed. For example, commercially available protease activatable probes targeting matrix metalloproteinases (MMPs) (MMPSense®, Perkin Elmer, Hopkinton, MA) have been widely used to illustrate enzyme activity in tumors and in other non-neoplastic diseases, such as stroke and arthritis.[17–19] In light of recent findings that NE mediates the upregulation of proinflammatory cytokines[13] and based on the knowledge that the local inflammatory response to PDT is also characterized by increased expression of several cytokines, including IL-1$\beta$, TNF-$\alpha$ and IL-6,[20] we performed an imaging study to characterize the NE enzyme activity in PDT-treated tumors using a newly developed NE-selective near infrared activatable optical probe, neutrophil elastase 680 FAST (NE680). We evaluated if PDT conditions that induce significant neutrophil accumulation in treated tumor sites alter local NE protease activity. We report that *in vivo* imaging results are consistent with significantly increased NE activity in PDT-treated tumors, and the extent of probe accumulation correlates with the magnitude of intratumor neutrophil influx associated with different treatment protocols.

## 2 Materials and methods

### 2.1 Animal and Tumor Models

Mouse mammary EMT6 tumors were initiated in the intradermal space on both of the hind legs of female BALB/c mice. Approximately 7 days after implantation, the tumors grew to a desired size of 7 to 10 mm in diameter. The more aggressive squamous cell carcinoma (SCC VII) tumors were grown intradermally on the right hind leg of C3H mice. The tumors reached a desired size of approximately 10 mm in diameter in 12 to 15 days. Both BALB/c and C3H mice were followed daily to track the tumor growth and were fed exclusively on a chlorophyll-free diet prepared to eliminate fluorescence originating from chlorophyll-derived compounds.

### 2.2 PDT Treatment Conditions

#### 2.2.1 Photofrin PDT

EMT6 and SCC VII tumors were subjected to PDT irradiation at 24 h following administration of 10 mg kg$^{-1}$ Photofrin via intravenous (IV) tail vein injection. Irradiation was performed using a 630 nm diode laser (RPMC Lasers, MO) at an irradiance of 100 mW cm$^{-2}$ for a fluence of 150 J cm$^{-2}$. This treatment protocol was based on previous studies, which evaluated different aspects of the inflammatory response elicited by Photofrin-PDT for this irradiation regimen.[5,21] The EMT6 tumor on the contralateral leg offered an unirradiated drug-only control. SCC VII tumors in C3H mice that did not receive Photofrin or that received Photofrin but were not irradiated [(+) drug, (−) light] were used as controls.

#### 2.2.2 HPPH PDT

To compare possible photosensitizer-specific differences in response, EMT6 tumors were also subjected to PDT sensitized with HPPH. HPPH (1 $\mu$mol kg$^{-1}$) was administered via tail vein

injection, and at 24-h postinjection, the tumor on one of the legs was irradiated using 667 nm light from a diode laser (Power Technology Inc., Little Rock, AR). Tumors were illuminated with a fluence of 100 J cm$^{-2}$ at an irradiance of 75 mW cm$^{-2}$. The choice of this treatment protocol was governed by a recent study by our group where we reported significant neutrophil influx in HPPH-PDT-treated tumors as visualized using *in vivo* confocal imaging.[7] Tumors on the contralateral leg offered an unirradiated, drug-only control.

### 2.3 NE680 Agent

NE680 was provided by PerkinElmer (Hopkinton, MA). Briefly, the NE selective probe consists of two NIR fluorophores (VivoTag-S680, PerkinElmer) that are linked to both the C- and N-termini of the peptide PMAVVQSVP, a highly NE-selective sequence.[22] The two fluorophores are placed in close enough proximity to each other for efficient quenching of fluorescence but become fluorescent upon cleavage of the substrate linker sequence. The linker sequence in the construct is designed to be preferentially cleaved by NE while remaining resistant to other proteases including mouse PR3.[22] This is important as both PR3 and NE are abundant serine proteases with potentially overlapping substrates.

### 2.4 Inhibition of NE

To establish that the observed increases in NE680 probe fluorescence were a consequence of cleavage of NE-selective sequence in the probe, *in vivo* studies were performed in the presence of a well-characterized NE inhibitor, Sivelestat (Tocris Bioscience, Ellisville, MO).[22,23] SCC VII and EMT6 tumors in C3H and BALB/c mice, respectively, were subjected to Photofrin-PDT and given 50 $\mu$l of 2 mg/ml Sivelestat via direct intratumor injection immediately after irradiation and 15 min prior to NE680 probe administration.

### 2.5 IVIS Imaging

Whole-mouse imaging was performed on an IVIS Spectrum system (PerkinElmer). Mice were anesthetized with ketamine/xylazine during the imaging procedure. Mice were first depilated using Nair to reduce autofluorescence from hair and placed in the imaging platform's enclosure. For NE680 imaging, 100 $\mu$l (4 nmols) of the probe was administered via tail vein injection, and imaging was performed at 5-h postadministration of the agent. In PDT-treated mice, the NE680 probe was injected immediately following irradiation. NE680 fluorescence was detected using a combination of 675 nm excitation and 720 nm emission bandpass filters with 30 and 20 nm bandwidths, respectively. The acquisition period ranged from 0.5 to 1 s. Images were processed and analyzed using Living Image 3.2 software (PerkinElmer). The fluorescence data are represented in terms of radiance efficiency, which automatically accounts for differences in acquisition variables among the images in an experimental set, such as integration time, $f$/stop, and pixel binning. The software also corrects for nonuniform excitation light over the field of view (FOV) on the sample stage by normalizing the fluorescence emission image to a reference image composed of reflected excitation light, stored as a library file in the analysis program.

To validate the observed patterns of *in vivo* NE680 fluorescence, *ex vivo* measurements were performed in excised SCC

VII tumor tissue from treated and control C3H mice. The skin and fat layers surrounding the excised tumor tissue were carefully stripped off, and the sample was washed to remove blood so as to minimize any effects of optical attenuation in the fluorescence measurements.

### 2.6  *Whole-Mount Immunofluorescence Imaging*

Whole-mount histology was performed by first excising the tumor and immediately immersing a small section of the tissue (15 to 20 mg) in an eppendorf tube. Prior to staining with antibodies, the samples were blocked using Fc Block (PharMingen, San Diego, CA) at 10 $\mu$g ml$^{-1}$ in 200 $\mu$l of phosphate buffered azide (PBA) (phosphate buffered saline $+0.1\%$ sodium azide) and placed on a rocker plate at 4°C for 20 min. Fluorophore-conjugated primary antibody was added directly to the tube at a predetermined concentration and incubated for an additional 90 min at 4°C. In order to label Gr1$^+$ cells in the tumor specimens, 50 $\mu$l of 0.05 mg ml$^{-1}$ anti-mouse Gr1 antibodies (clone RB6-8C5; Biolegend, San Diego, CA) conjugated to Alexa Fluor 488 was added. Following this incubation period, the antibody plus PBA solution was aspirated, and the tumor sample was washed twice by adding 1 ml of PBA to the tube and shaking it on the rocker at 4°C for 45 min. After the final wash, samples were removed from the tubes and placed between microscopy grade coverslips using a home-built device that enabled imaging of whole-mount preparations.[24] The fluorophore Alexa Fluor 488 was excited at 488 nm from an argon ion laser and detected using a combination of 500-nm longpass and 515/30 nm bandpass filters (Chroma Technology, Bellows Falls, VT). The combination of a 100-$\mu$m-diameter pinhole and a 10×, 0.45 numerical aperture objective gave a 6-$\mu$m optical section thickness. The images were acquired at 16 bits with a lateral resolution of 1 $\mu$m/pixel. In order to construct confocal images of larger areas of excised tumor fragments, a computer-controlled motorized stage (BioPrecision2 stage, Ludl Electronics Product Ltd., Hawthorne, NY) with a linear encoder resolution of 50 nm was used. A Labview (National instruments Corp., Austin, TX) based image acquisition software allowed translation of the stage and acquisition of 600 × 600 $\mu$m$^2$ individual fields that were stitched using ImageJ to create a mosaic with a FOV of 3.6 × 2.4 mm$^2$. The images were analyzed using ImageJ 1.43u, a public domain image processing software distributed by the NIH (http://rsbweb.nih.gov/ij/). The detailed procedures of the analysis have been reported previously.[7]

## 3  Results and Discussion

In a study reported by Sun et al.,[5] the authors examined the activity of neutrophils in SCC VII tumors subjected to Photofrin-PDT by assaying for tumor levels of neutrophilic myeloperoxidase (MPO). MPO, a neutrophil-specific enzyme, is released extracellularly upon cell activation and is considered an indicator of neutrophil-mediated cytotoxicity during inflammatory responses. The treatment protocol involved an intravenous administration of 10 mg kg$^{-1}$ Photofrin followed by illumination with 120 mW cm$^{-2}$ at 630 nm after a drug-light interval of 24 h. This treatment regimen resulted in a significant and sustained release of MPO into the tumor interstitium, with increased levels detectable as early as 2 h and reaching maximum enhancement at 8- to 13-h postirradiation. The findings from this report not only provided a rationale to investigate NE, another member of the neutrophil-associated enzyme family, but also informed the choice for the Photofrin-PDT protocol and the time point for NE imaging adopted for this current study.

*In vivo* whole-mouse fluorescence imaging using the IVIS Spectrum imager showed that the NE680 fluorescence was greatly enhanced in SCC VII tumors subjected to Photofrin-PDT [Fig. 1(c)] relative to controls [Fig. 1(a) and 1(b)]. As described in Sec. 2, the NE680 probe was injected in treated mice immediately following irradiation, and imaging was performed 5 h later. Thus, assuming that the cleaved probe does not clear on this time scale, NE680 levels imaged in PDT-treated tumors reflect cumulative elastase enzyme activity during the initial 5-h postirradiation. A quantitative comparison among the different groups was performed by measuring the fluorescence signal from a region of interest drawn over tumor regions of the mouse [Fig. 2(a)]. The NE680 fluorescence measured from Photofrin-PDT-treated SCC VII tumors was approximately threefold to fourfold higher than that measured in control tumors ($n = 3$ for each group). The difference in fluorescence intensity between the untreated and drug-only control tumors was not statistically significant. In these controls, the source of observed NE680 fluorescence may be attributed to constitutive levels
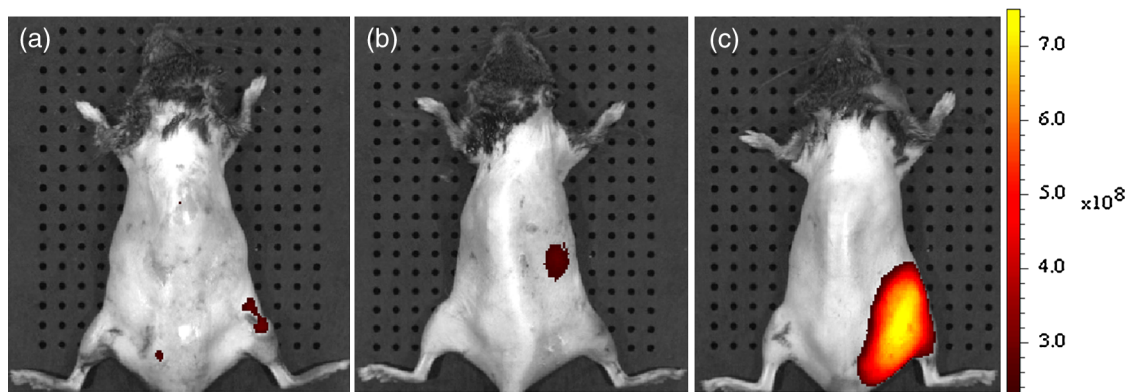


**Fig. 1** Whole-mouse fluorescence images of neutrophil elastase (NE) activity in SCC VII tumors established on the right hind leg of C3H mice. (a) Control [(−) drug (−) light], (b) Unirradiated drug-only control [(+) drug (−) light] and (c) Photofrin-PDT treated [(+) drug (+) light]. 10 mg kg$^{-1}$ Photofrin was injected intravenously, and irradiation was performed 24 h later with a fluence of 150 J cm$^{-2}$ at an irradiance of 100 mW cm$^{-2}$. Immediately after irradiation, 100 $\mu$l of NE680 probe was administered via tail vein injection. Imaging was performed 5 h later on an IVIS Spectrum system. NE680 was excited and detected with a combination of 675/30 and 720/20 nm filters, respectively. The color bar represents radiance efficiency.
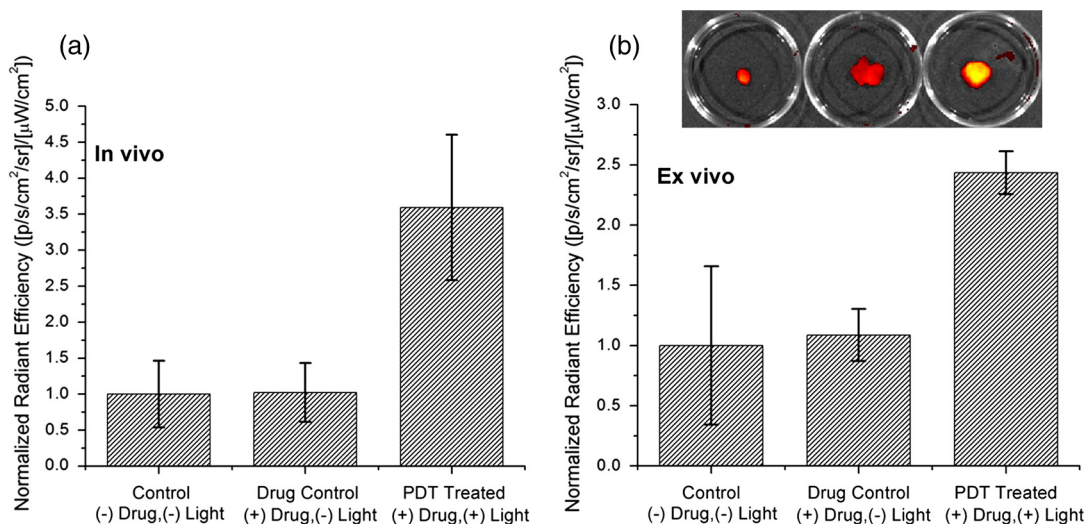
**Fig. 2** (a) Quantitative image analysis of *in vivo* NE680 fluorescence levels measured from region of interests assigned over tumor sites on the mice (*n* = 3 for each group). (b) *Ex vivo* NE680 levels measured in excised tumor tissue (*n* = 2) using the IVIS system. Data are normalized to intensities in control tumor samples. The representative images in the inset illustrate the intensities on the same color scale for representative control (left), unirradiated drug-only control (center), and Photofrin-PDT-treated (right) tumor specimens.

of NE present in a tumor. The differences observed *in vivo* in tumoral NE680 probe activation were further investigated by measurements in excised tumor samples [Fig. 2(b)], which are not influenced by possible treatment-induced changes in overlying skin. Interestingly, the *ex vivo* NE levels in treated SCC VII tumors (*n* = 2) were found to be approximately 2.5-fold greater than those in controls. This slightly lower level of enzyme activity in excised tumors may suggest a significant activation of neutrophils in the skin immediately adjacent to the tumor *in vivo*.

Figures 3 and 4 illustrate NE activity in EMT6 tumors established in BALB/c mice. Fluorescence measured from any activatable probe at a target site includes contributions from a combination of probe delivery and activation. Therefore, measurement of NE680 intensity in an unirradiated tumor in the contralateral leg offers an important internal control in that it is not influenced by variations in intravenous probe administration. Consequently, any fluorescence enhancement observed in treated versus unirradiated tumors is most likely due to PDT-induced changes in elastase activity. Figure 3(a) shows a representative image of NE680 fluorescence acquired from an EMT6 tumor subjected to Photofrin-PDT. The tumor on the contralateral leg was not irradiated and exhibits fluorescence intensity that is below the lower threshold of the display scale. The data from unirradiated and irradiated EMT6 tumors (*n* = 3 for each group) are summarized in Fig. 3(b) and show that
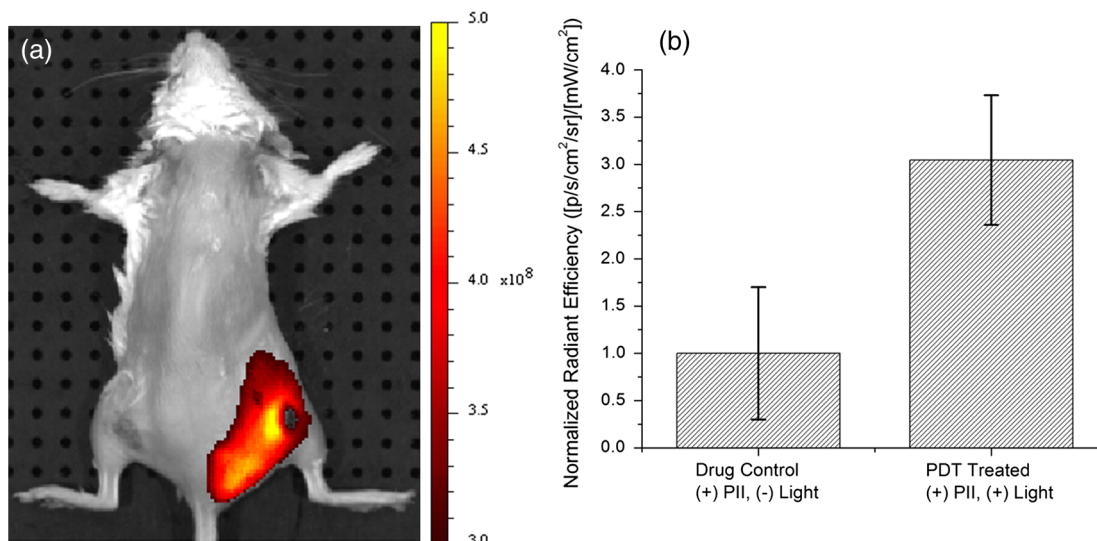


**Fig. 3** (a) Representative whole-mouse fluorescence image of NE activity in EMT6 tumors established in both hind legs of a BALB/c mouse. The tumor on the right leg was subjected to illumination, whereas the tumor on the left leg was shielded from any light exposure, thereby providing a Photofrin-sensitized, unirradiated control. 10 mg kg$^{-1}$ Photofrin was injected intravenously, and irradiation on the right leg tumor was performed 24 h later with a fluence of 150 J cm$^{-2}$ at an irradiance of 100 mW cm$^{-2}$. Immediately after irradiation, 100 $\mu$l of NE680 probe was administered, and imaging on the IVIS system was done 5 h later. (b) Quantitative comparison of NE680 fluorescence in irradiated versus unirradiated control tumors (*n* = 3 for each group). Data are normalized to intensities in unirradiated drug-only control tumor samples. Error bars represent standard deviation.
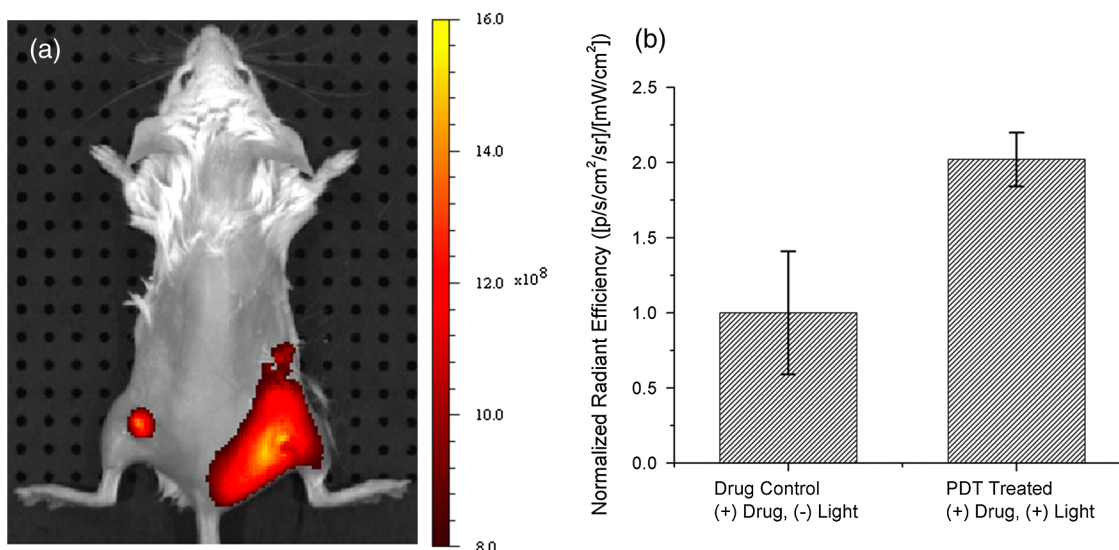
**Fig. 4** (a) NE680 fluorescence image acquired from a BALB/c mouse with bilateral EMT6 tumors. The tumor on the right leg was subjected to illumination, whereas the tumor on the left leg was shielded from light exposure and served as an HPPH-sensitized, unirradiated control. HPPH (1 1 $\mu$mol kg$^{-1}$) was injected intravenously, and irradiation was performed 24 h later with a fluence of 100 J cm$^{-2}$ at an irradiance of 75 mW cm$^{-2}$. Five hours following irradiation and NE680 administration, whole-mouse imaging was performed. (b) Quantitative comparison of NE680 fluorescence in irradiated versus unirradiated control tumors ($n = 3$ for each group). Data are normalized to intensities in unirradiated drug-only control tumor samples. Error bars represent standard deviation.

Photofrin-PDT induces an enhancement of NE activity by at least threefold at 5-h postirradiation. These results obtained from EMT6 tumors are remarkably similar to those observed in SCC VII tumors (Fig. 2).

Figure 4 exhibits data from EMT6 tumors ($n = 3$) subjected to HPPH-PDT. In the whole-mouse image of Fig. 4(a), in addition to an increased level of NE680 induced by irradiation, there is also an evidence of some upregulation of elastase activity in the unirradiated tumor. This suggests the possibility that intratumoral HPPH drug accumulation stimulates a modest increase in neutrophil activation and consequent NE release. The summary data plot in Fig. 4(b) shows that NE680 fluorescence is approximately twofold higher in treated versus unirradiated tumors, which is significantly lower than the threefold difference observed with Photofrin-PDT.

In order to verify that the enhanced levels of NE680 fluorescence measured in irradiated tumors relative to unirradiated controls were caused by increased elastase activity and cleavage

of the probe, we performed *in vivo* experiments to examine the attenuation of NE function in irradiated tumors with the introduction of an established NE inhibitor. Sivelestat is a selective NE inhibitor and has been shown to be effective clinically in mitigating the effect of systemic inflammatory response in patients with acute lung injury.[25] PDT-treated tumors that received Sivelestat via intratumor injection were assayed for NE680 fluorescence, and the levels were compared to those obtained from unirradiated and irradiated tumors in the absence of Sivelestat. Figure 5(a) shows significant inhibition of NE activity upon administration of Sivelestat into SCC VII tumors subjected to Photofrin-PDT. The introduction of the inhibitor resulted in decreased NE680 fluorescence to intensities observed in unirradiated drug-only control tumors. The presence of Sivelestat in Photofrin-PDT-treated EMT6 tumors also diminished the NE680 fluorescence from their levels observed in irradiated tumors [Fig. 5(b)]. The NE680 levels between unirradiated drug-only control and irradiated plus
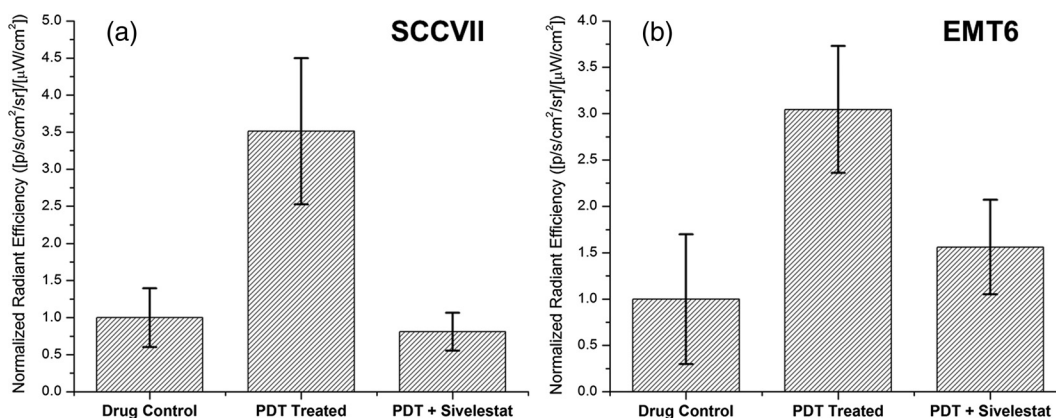


**Fig. 5** Comparison of NE680 fluorescence levels in (a) SCC VII and (b) EMT6 tumors among three groups: Photofrin-sensitized but unirradiated (drug control), subjected to irradiation (PDT treated) and irradiated plus administered the NE inhibitor, Sivelestat (PDT+Sivelestat). Sivelestat was delivered via direct intratumor injection 15 min prior to NE680 administration in the mice. Data are normalized to intensities in unirradiated drug-only control tumor samples. Error bars represent standard deviation.
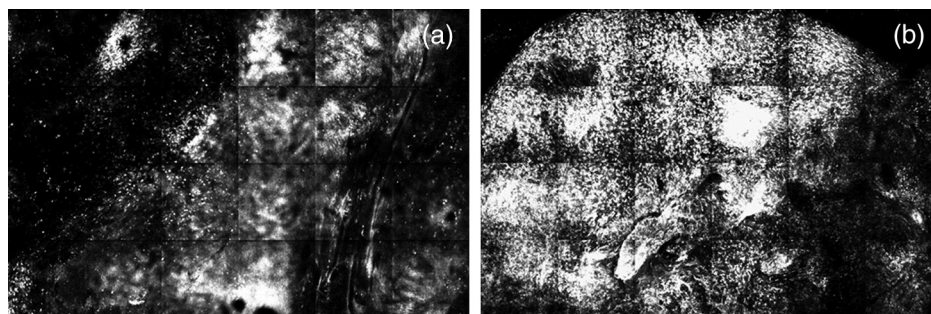
**Fig. 6** Confocal fluorescence images of Alexa488-conjugated anti-Gr1+ labeled cells in tissue fragments excised from EMT6 tumors in BALB/c mice. (a) Control tumor that received Photofrin but was not irradiated, and (b) tumor that was PDT treated and excised 5-h postirradiation. The FOV imaged in both of these tumors is $3.6 \times 2.4$ mm$^2$, constructed from a montage of 24 individual $600 \times 600$ $\mu$m$^2$ fields. The Gr1+ cell counts in Photofrin-PDT-treated tumor tissue are at least 10-fold greater than that in the unirradiated drug-only control tissue.

Sivelestat groups for both SCC VII and EMT6 tumors were not different at the $P = 0.1$ significance level. Kossodo et al.[22] performed a number of corroborating studies to extensively characterize the NE680 probe and verified that the dominant protease involved in probe cleavage is NE, and no other neutrophil- or nonneutrophil-associated proteases. Our own findings and that of Kossodo et al., therefore, strongly suggest that measured changes in NE680 probe fluorescence is a readout of corresponding variations in intratumoral NE activity.

In order to interpret the difference in the extent of NE680 enhancement observed with Photofrin- versus HPPH-PDT treatment regimens, we evaluated neutrophil influx into PDT-treated tumors sensitized with Photofrin versus HPPH. We have recently reported on the use of confocal imaging to visualize populations of Gr1+ cells and MHC-II+ antigen presenting cells in tumors subjected to HPPH-PDT.[7] The HPPH-PDT treatment conditions were identical to those used in this study. We found that HPPH-PDT results in 1.5- and 2.5-fold increase in intratumoral accumulation of Gr1+ cells at 5-h and 24-h postirradiation, respectively. To assay for Photofrin-PDT-induced influx of Gr1+ cells, we used whole-mount labeling of *ex vivo* tissues obtained from control and treated tumors. Figure 6(a) and 6(b) show fluorophore-labeled infiltrating Gr1+ cells imaged in an unirradiated control and PDT-treated tumor specimen, respectively. The tissue fragment illustrated in Fig. 6(b) was excised from a treated tumor at 5-h postirradiation. Each image is comprised of twenty-four $600 \times 600$ $\mu$m$^2$ individual fields, which were stitched to create a montage with a FOV of $3.6 \times 2.4$ mm$^2$, as described in Sec. 2. Analysis of the images revealed that the influx of Gr1+ cells into Photofrin-PDT-treated EMT6 tumors was at least 10 times greater than that measured in unirradiated drug-only control tumors ($n = 2$ for each group). The cell densities were found to be similar in Photofrin-PDT-treated tumor tissues excised at 5-h and 24-h postirradiation (data not shown). These results are qualitatively consistent with those reported by Sun et al.,[5] who observed a 10-fold increase in accumulated neutrophils in Photofrin-PDT treated versus untreated SCC VII tumors, as measured indirectly via MPO assay. Gollnick et al.[26] reported that the number of infiltrating neutrophils were considerably fewer following HPPH- versus Photofrin-PDT. The authors attributed the results to the lower degree of inflammation associated with HPPH-PDT (Ref. 27) and to the kinetics of tumor destruction, with tumor regression occurring within 24 h after Photofrin-PDT versus a prolonged period of 72 to 96 h with HPPH-PDT. As NE is an enzyme released from neutrophil granules upon activation, it is therefore likely that the stronger inflammatory response triggered by Photofrin-PDT contributes to increased elastase activity imaged in irradiated tumors sensitized with Photofrin versus HPPH.

In conclusion, this study was motivated by recent reports that highlight the extended functions of neutrophils and their downstream effects in mounting both innate and adaptive host response.[10] Serine proteases released from activated neutrophils have emerged as a major player in the regulation of inflammatory response, such as specifically altering the function of cytokines and chemokines.[11] Mittendorf et al.[28] recently showed that a novel breast cancer antigen, Cyclin E, is cleaved after specific uptake of NE by breast cancer cells, and this increases the susceptibility of the cancer cells to lysis by cytotoxic T lymphocytes-specific for the antigen. This novel observation along with other recent findings therefore demonstrates that extracellularly released NE has physiologic functions that contribute to host defense, and hence the conventional view that assigns NE as pathogenic for tissue-destructive diseases, such as acute or chronic pulmonary diseases, warrants careful reassessment.[13,28] Further, as PDT induces increased accumulation of neutrophils in treated tumors and NE is released from activated neutrophils and stimulates proinflammatory cytokines, our characterization of significant NE increase in PDT-treated tumors establishes a rationale to further evaluate a previously undescribed role of NE in linking the elements of innate and adaptive host response associated with PDT.

## References

1. P. Agostinis et al., "Photodynamic therapy of cancer: an update," *CA Cancer J. Clin.* **61**(4), 250–281 (2011).

2. M. Korbelik, "PDT-associated host response and its role in the therapy outcome," *Lasers Surg. Med.* **38**(5), 500–508 (2006).
3. W. J. de Vree et al., "Evidence for an important role of neutrophils in the efficacy of photodynamic therapy in vivo," *Cancer Res.* **56**(13), 2908–2911 (1996).
4. P. C. Kousis et al., "Photodynamic therapy enhancement of antitumor immunity is regulated by neutrophils," *Cancer Res.* **67**(21), 10501–10510 (2007).
5. J. Sun et al., "Neutrophils as inflammatory and immune effectors in photodynamic therapy-treated mouse SCC VII tumours," *Photochem. Photobiol. Sci.* **1**(9), 690–695 (2002).
6. T. H. Foster et al., "Intratumor administration of the photosensitizer Pc 4 affords photodynamic therapy efficacy and selectivity at short drug-light intervals," *Transl. Oncol.* **3**(2), 135–141 (2010).
7. S. Mitra, O. Mironov, and T. H. Foster, "Confocal fluorescence imaging enables noninvasive quantitative assessment of host cell populations in vivo following photodynamic therapy," *Theranostics* **2**(9), 840–849 (2012).
8. M. Korbelik and I. Cecic, "Contribution of myeloid and lymphoid host cells to the curative outcome of mouse sarcoma treatment by photodynamic therapy," *Cancer Lett.* **137**(1), 91–98 (1999).
9. S. O. Gollnick and C. M. Brackett, "Enhancement of anti-tumor immunity by photodynamic therapy," *Immunol. Res.* **46**(1–3), 216–226 (2010).
10. A. Mantovani et al., "Neutrophils in the activation and regulation of innate and adaptive immunity," *Nat. Rev. Immunol.* **11**(8), 519–531 (2011).
11. U. Meyer-Hoffert and O. Wiedow, "Neutrophil serine proteases: mediators of innate immune responses," *Curr. Opin. Hematol.* **18**, 19–24 (2011).
12. C. T. Pham, "Neutrophil serine proteases: specific regulators of inflammation," *Nat. Rev. Immunol.* **6**(7), 541–550 (2006).
13. R. Benabid et al., "Neutrophil elastase modulates cytokine expression: contribution to host defense against pseudomonas aeruginosa-induced pneumonia," *J. Biol. Chem.* **287**(42), 34883–34894 (2012).
14. J. O. McIntyre and L. M. Matrisian, "Molecular imaging of proteolytic activity in cancer," *J. Cell Biochem.* **90**(6) 1087–1097 (2003).
15. R. Weissleder et al., "*In vivo* imaging of tumors with protease-activated near-infrared fluorescent probes," *Nat. Biotechnol.* **17**(4), 375–378 (1999).
16. M. Solomon et al., "Detection of enzyme activity in orthotopic murine breast cancer by fluorescence lifetime imaging using a fluorescence resonance energy transfer-based molecular probe," *J. Biomed. Opt.* **16**(6), 066019 (2011).
17. J. Baeten et al., "*In vivo* investigation of breast cancer progression by use of an internal control," *Neoplasia* **11**(3), 220–227 (2009).
18. P. A. Barber et al., "Infrared optical imaging of matrix metalloproteinases (MMPs) up regulation following ischemia reperfusion is ameliorated by hypothermia," *BMC Neurosci.* **13**(76), 76 (2012).
19. E. F. Jones et al., "Characterization of human osteoarthritic cartilage using optical and magnetic resonance imaging," *Mol. Imag. Biol.* **14**(1), 32–39 (2012).
20. A. P. Castano, P. Mroz, and M. R. Hamblin, "Photodynamic therapy and anti-tumour immunity," *Nat. Rev. Cancer*, **6**(7), 535–545 (2006).
21. G. Krosl, M. Korbelik, and G. J. Dougherty, "Induction of immune cell infiltration into murine sccvii tumour by photofrin-based photodynamic therapy," *Br. J. Cancer* **71**(3), 549–555 (1995).
22. S. Kossodo et al., "Noninvasive in vivo quantification of neutrophil elastase activity in acute experimental mouse lung injury," *Int. J. Mol. Imag.* **2011**, 581406 (2011).
23. S. Miyoshi et al., "Usefulness of a selective neutrophil elastase inhibitor, sivelestat, in acute lung injury patients with sepsis," *Drug Des. Devel. Ther.* **7**, 305–316 (2013).
24. S. A. Gerber et al., "Preferential attachment of peritoneal tumor metastases to omental immune aggregates and possible role of a unique vascular microenvironment in metastatic survival and growth," *Am. J. Pathol.* **169**(5), 1739–1752 (2006).
25. N. Aikawa et al., "Reevaluation of the efficacy and safety of the neutrophil elastase inhibitor, sivelestat, for the treatment of acute lung injury associated with systemic inflammatory response syndrome; a phase IV study," *Pulm. Pharmacol. Ther.* **24**(5), 549–554 (2011).
26. S. O. Gollnick et al., "Altered expression of interleukin 6 and interleukin 10 as a result of photodynamic therapy in vivo," *Cancer Res.* **57**(18), 3904–3909 (1997).
27. D. A. Bellnier et al., "Murine pharmacokinetics and antitumor efficacy of the photodynamic sensitizer 2-[1-hexyloxyethyl]-2-devinyl pyropheophorbide-a," *J. Photochem. Photobiol. B* **20**(1), 55–61 (1993).
28. E. A. Mittendorf et al., "Breast cancer cell uptake of the inflammatory mediator neutrophil elastase triggers an anticancer adaptive immune response," *Cancer Res.* **72**(13), 3153–3162 (2012).